DYNAMICAL MODELING AND CONTROL DESIGN OF A FLEXIBLE RADAR ANTENNA

Agenor de Toledo Fleury, agfleury@fei.edu.br
Centro Universitário da FEI
Av. Humberto de Alencar Castelo Branco, 3972 – 09850-901, São Bernardo do Campo, S.P.
Escola Politécnica da Universidade de São Paulo
Av. Prof. Mello Moraes, 2253 – 05508-900, São Paulo, SP

Fabrizio Leonardi, fabrizio@fei.edu.br
Centro Universitário da FEI
Av. Humberto de Alencar Castelo Branco, 3972 – 09850-901, São Bernardo do Campo, S.P.

Fabiano Armellini, **armellini@allagi.com.br**
Allagi Engenharia Ltda
Av. Brigadeiro Faria Lima, 1461 - Cj 124 –01452-002 - São Paulo - SP

Abstract. A radar antenna is basically composed of a primary source mounted at the focal point of a parabolic reflector. The radar illumination rule is established so that the desired beam shape is attained as precisely as possible. The mechanical movement of the set reflector-pedestal must be designed to fit the desired volume of radar exploitation. This work deals with the design of a 4.2m-diameter large, flexible, rotating radar antenna prototype, , already operating in Mogi das Cruzes, SP, under the supervision of the Brazilian Omnisys/Atech joint venture. A Finite Element structural model of the reflector-pedestal has been proposed, analysed and compared to experimental data to generate a model suitable for control design. Based on this model, some control approaches have been used to get good answers for the antenna in the presence of wind or other type of perturbations.

Keywords: structural dynamics; finite element models; singular perturbations method; classical control methods

1. INTRODUCTION

In a broad sense, radars may be classified as electronic sensors that use electromagnetic waves to detect objects and measure relative positions in space. Object positioning is accomplished by determining distance and attitude in relation to the radar equipment, which requires three coordinates: azimuth (around the vertical axis), elevation (around the horizontal axis) and the straight distance from the pointing equipment. This distance-azimuth-elevation set of measurements constitutes a spherical coordinate system with the radar antenna focal point in the origin, as shown in Figure 1.
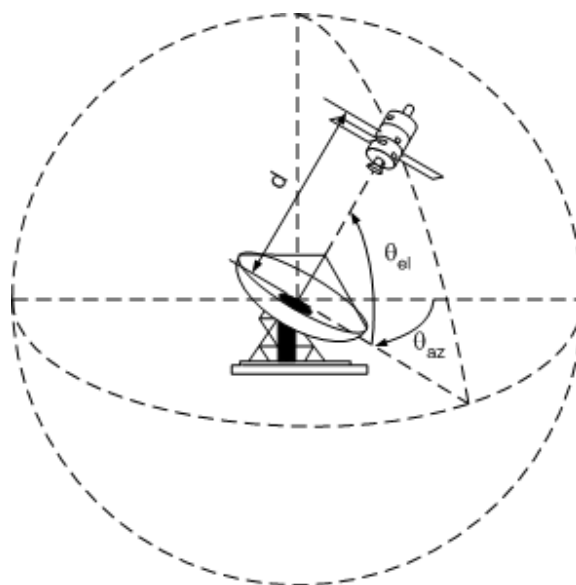

Figure 1 – Radar as the center of a spherical coordinate system.

Distance between target and radar is determined using the Pulse-Echo Principle in which a high power electromagnetic pulse is sent in a given direction and target distance is calculated by the signal delay (echo) from the

target. The other coordinates, azimuth and elevation, are given by the angular position of the antenna-radar set relative to a fixed reference.

This work deals with velocity and position control of a large radar antenna using a two-axes gimbal of the type elevation over azimuth. Each axis performs independent motion driven by a DC brushless motor. Both are digitally controlled by a central processing system. The antenna-radar set described here is the mechatronic part of a large project that qualified Atmos (the spinoff of the Atech-Omnisys joint venture) to design and build weather radars to Brazilian authorities. The paper is based on the MSc work by Armellini (2006) where a detailed description can be found. Here, some basic concepts on radar design are addressed, the essential requirements for mechanical and control design are presented and results for taking into account the flexibility of a large rotating structure are shown and discussed.

2. RADAR DESIGN CONCEPTS

The quality of information received by an antenna depends on its angular velocity, pointing accuracy, radar pulse parameters and electronic gain, angular aperture, antenna lobes and beam shape features. These electronic parameters and the antenna polarization define the radar structural properties: reflector shape (parabolic or semi-parabolic, for example), geometry (diameter and curvature of the dish) and primary source location over the reflector (focal distance, vertical or horizontal or circular polarization). One of the major difficulties in nowadays development design projects is to combine mechanical and electrical designs to guarantee information accuracy with increasing antenna gains. Gain increase leads to larger reflectors and, consequently, to mechanical structures of complex dynamic behaviors which present several complex flexibility and vibration issues to be dealt with (Armellini, 2006). It is a task of the control system to attenuate them.

There are several different configurations for the antenna support and movement. For this project, a standard two-axis elevation-over-azimuth (EL/AZ) positioner was adopted. This configuration, also known as theodolite assembly, is shown in Figure 2.
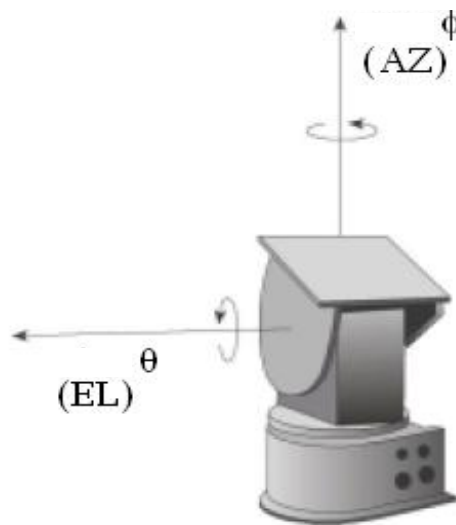

Figure 2 – Elevation over azimuth (EL/AZ) assembly.

For radars in general, positioner motion and velocity control represents a crucial feature since the radar must sweep all the aerial space around itself with a very narrow illuminating beam. For weather radars, in particular, trajectories must be prescribed and accurately tracked for cloud and other meteorological phenomena real detection.

3. ANTENNA CONTROL BACKGROUND

Radar design has evoluted in parallel to control systems. In the 30's, mechanical servomechanisms were used to multiply input torques necessary to move the antenna at the output axis while making null the angular error. Modern configurations, as the one shown in Figure 3, still use the same basic idea.

Each pointing mechanism is controlled by an independent loop. For the task of control, azimuth and elevation loops are somewhat identical. They differ on the mechanical parameters like inertias and stiffness, displacement bumps or controller gains. Both loops have an internal circuit as required for DC brushless type motors. The scheme in Figure 3 shows also a special block to take into account the existence of safety interlock circuits associated to temperature sensors, locking keys and so on, necessary to protect the equipment against equipment damage and human hazard.
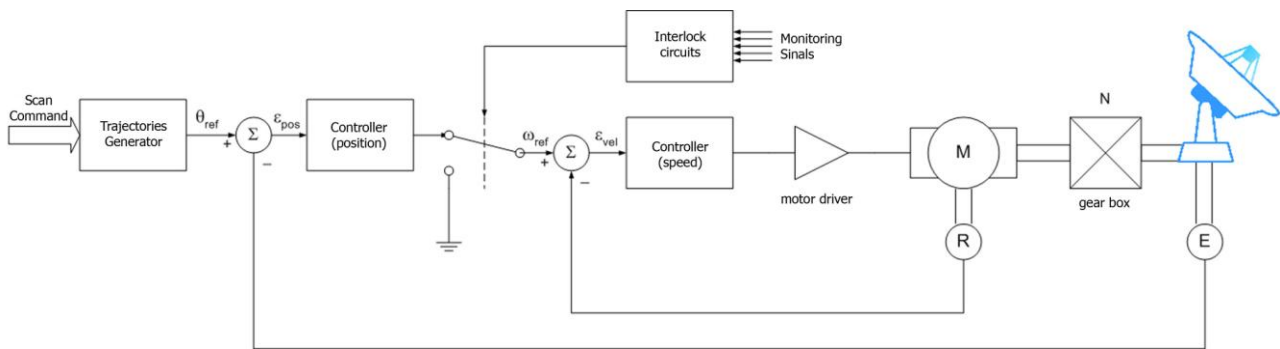
Figure 3 – Control loop scheme.

On the other side, as antennas grow larger, the importance of system flexibilities grows in parallel. These flexibilities are due to dishes, gimbals, support structures, axles and cannot be neglected in a good design. Baek (2006) reinforces this statement when modeling an azimuth driving servo system carrying a flexible antenna. Major part of the elastic Degrees of Freedom (DOF) are assigned inside the gimbals (axles and gears) and a simple beam model is adopted for the antenna when trying to match model responses to experimental modal analysis results. Gawronski (2006) proposes that the most important measure of control performance is the error while tracking under wind gusts and compares parameter sensitivities for a rigid antenna under a PI controller and a large flexible dish using a LQG strategy to conclude that the first approach gives better simulation results. This is not surprising since flexible modes require much more accurate controllers. Problem is how to design a large mechanical system that can be considered rigid in all circumstances.

In this work, the weather radar is modeled as a flexible low order system and unknown parameters are adjusted to cope with the structural analysis results. Based on this model, PID and LQ controllers for the azimuth axis are designed and their performances compared.

4. NUMERICAL AND EXPERIMENTAL STRUCTURAL ANALYSIS

The prototype weather radar antenna is a 4,2m diameter parabolic dish built of aluminum alloy. All other parts are made of steel, including counterweights, as can be seen in Figure 4. The radar set is installed at the top of a 12m-high steel tower, as shown in Figure 5. This Figure gives an idea of the test site, located in Mogi das Cruzes, SP. The building at left, in Figure 5, houses all the electronic modules inside a climate controlled room.

Figure 4 – Lateral View of the Prototype Weather Radar (Armellini,2006)

Figure 5 – Test site in Mogi das Cruzes, SP (Armellini, 2006)

A Finite Element model of gimbals and dish, not including tower, has been implemented on an ANSYS 8.1 package. The resulting model has somewhat 45,000 nodes and 246,000 DOF's (Armellini, 2006) and the main frequencies and modes between 0 and 50 Hz were achieved. Numerical analysis showed 13 frequencies below 20 Hz, the first on 5.4 Hz, corresponding to elevation axis torsion mode and the second on 9.6 Hz relative to the azimuth axis torsion mode. These two modes are shown in Figure 6.
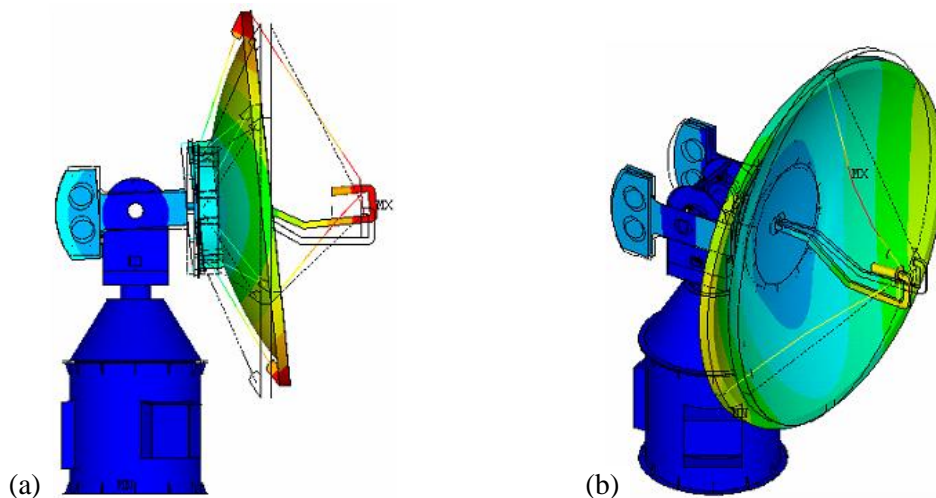

Figure 6 – First 2 Vibration Modes: (a) torsion of the elevation axis; (b) torsion of the azimuth axis

The Experimental Modal Analysis was performed with the radar set installed at the tower. First mode has been confirmed at 5.5 Hz but surprisingly the apparatus has shown 2 modes around 1.2 Hz in the azimuth direction and in the North (azimuth and elevation) direction. This fact seems to be associated to the tower resonance frequencies, but a deeper investigation still remains to be performed.

5. AZIMUTH CONTROL SYSTEM DESIGN

In what follows, azimuth and elevation dynamics are assumed independent, which allows one to treat the system as two different problems. In this scenario, interactions between the two axes are modeled as disturbances. This work deals only with the azimuth angle control since this is considered the critical axis (Baek, 2006).

The dynamic model includes some uncertain parameters, therefore the controller must be robust to these modeling uncertainties. QFT controllers are recommended compensators for cases like this (Houpis, 1999). However, since the current model is only a preliminary one and available data do not allow outlining uncertainties correctly, robustness was

not considered explicitly. In spite of this, one tried to provide some degree of implicit robustness regarding the real application.

As a constraint to the problem, the compensator must have a specific structure since the real system is equipped with a PID controller. To provide an optimal solution, one decided to design a Linear Quadratic Regulator (LQR) and then map the resulting control law to a PID structure which, under some circumstances, can approximate the optimal control law.

To investigate a system, it is mandatory to build a complete and rigorous model. However, the model normally can be less detailed for control purpose if the controller is robust in presence of modeling uncertainties. Based on this assumption, one adopts a linear model to represent all antenna dynamics. In order to represent the antenna flexibility, spring and damper elements have been associated to every degree of freedom. Figure 7 presents a simplified scheme for the radar, where 'm' identifies the degree of freedom of the motor, 'g' the gimbal and 'a' the antenna.
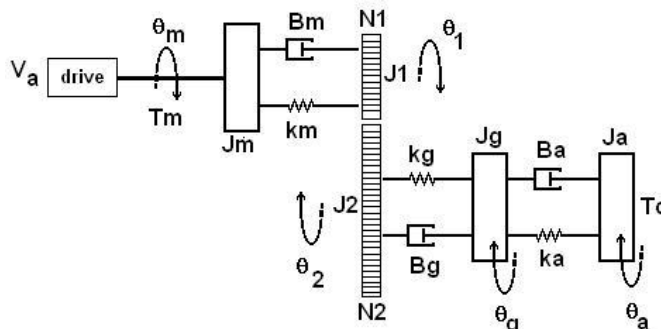

Figure 7 – Physical Model of the Radar System.

Equation 1 shows the linear mathematical system associated to the model above, disregarding the inertia moments of the mechanical gear box. Some of the model parameters were obtained from the structural simulation. The motor parameters are well known, but the other parameter values have been adjusted in order to match responses of the known system behavior, as the natural frequencies of the first vibration modes.

$$J_m \ddot{\theta}_m(t) = k_M i_a(t) - k_m \left(\theta_m(t) - \theta_1(t)\right) - B_m \left(\dot{\theta}_m(t) - \dot{\theta}_1(t)\right)$$

$$0 = -k_m \left(\theta_1(t) - \theta_m(t)\right) - B_m \left(\dot{\theta}_1(t) - \dot{\theta}_m(t)\right) - \frac{1}{N}\left[k_g\left(\frac{1}{N}\theta_1(t) - \theta_g(t)\right) + B_g\left(\frac{1}{N}\dot{\theta}_1(t) - \dot{\theta}_g(t)\right)\right]$$

$$J_g \ddot{\theta}_g(t) = -k_g\left(\theta_g(t) - \frac{1}{N}\theta_1(t)\right) - B_g\left(\dot{\theta}_g(t) - \frac{1}{N}\dot{\theta}_1(t)\right) - k_a\left(\theta_g(t) - \theta_a(t)\right) - B_a\left(\dot{\theta}_g(t) - \dot{\theta}_a(t)\right)$$

$$J_a \ddot{\theta}_a(t) = T_c(t) - k_a\left(\theta_a(t) - \theta_g(t)\right) - B_a\left(\dot{\theta}_a(t) - \dot{\theta}_g(t)\right)$$

$$L_a \dot{i}_a(t) = V_a(t) - R_a i_a(t) - K_E \dot{\theta}_m(t) \tag{1}$$

The parameter values used for system simulation and design are those shown in Table 1.

Table 1. Parameter values.

Antenna moment of inertia J_a	660 kg.m^2
Antenna stiffness K_a	5.8625e+6 N.m/rad
Antenna damping B_a	886.7 N.m.sec/rad
Gimble moment of inertia J_g	1500 kg.m^2
Gimble stiffness K_g	9.59e+6 N.m/rad
Gimble damping B_g	5.25539e+3 N.m.s/rad
Motor moment of inertia J_m	3.78e-3 kg.m^2
Motor stiffness K_m	34125 N.m/rad
Motor damping B_m	1.1357486 N.m.sec/rad
Motor constant of torque K_M	0.56 N.m/A
Motor emf constant K_E	0.45 V.sec/rad
Motor resistance R_a	0.56 Ω
Motor Inductance L_a	3.78e-3 H
Mechanical reduction N	464.4

With these values, the state space model derived from Equation (1) results badly conditioned because of the high numeral range of the elements in the dynamic matrix. This occurs mainly due to the reduced values of the motor parameters compared to the antenna ones, fact that brings numerical problems reflected in the ratio of the smallest to the largest value of system eigenvalues. To improve system conditioning, the fastest pole, about 1000 times faster than others, was removed from the model and the slower one was moved to the origin, once the system output is the angular position.

Figure 8 shows the Bode diagrams of the model with those adjustments (7 states), in comparison to the original model (8 states). Notice that there is no loose of relevant information in the range of frequencies of 0,1 rad/sec to 1000 rad/sec, that is, in the range of practical interest.
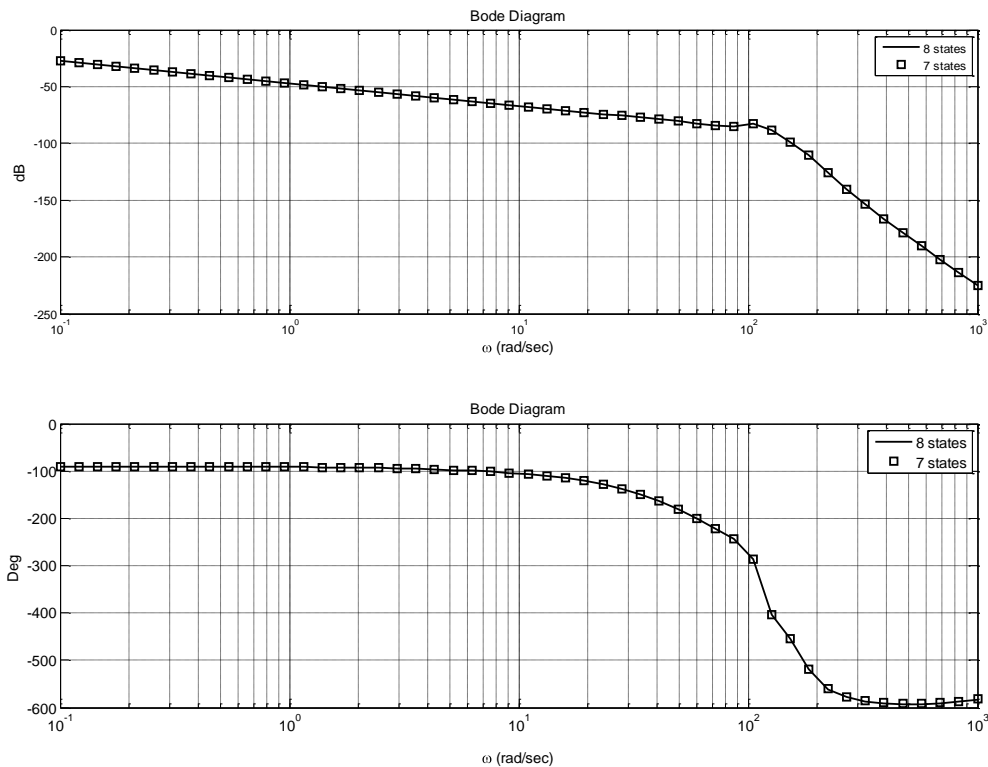

Figure 8 – Bode Diagrams of the Reduced Order and Original Models.

An integrator in the direct path is necessary if system output must track a constant reference signal with null stationary error. However, to reject a constant disturbance signal with no stationary error either, it is necessary to provide the controller with an internal integrator, even if an integrator already exists in the plant model. In this application, since both, the servo and the regulatory problems, are important, a new integrator is added to the plant for the design purposes. In a SISO system, this integrator can be added to plant input or to plant output, but in multivariable cases it is recommended to add it (or them) to the output in order to avoid that the state feedback push it (or them) out of the origin. The new state space representation becomes

$$\begin{bmatrix} \dot{x}(t) \\ \dot{z}(t) \end{bmatrix} = \begin{bmatrix} A & 0 \\ C & 0 \end{bmatrix} \begin{bmatrix} x(t) \\ z(t) \end{bmatrix} + \begin{bmatrix} B \\ 0 \end{bmatrix} u(t) \tag{2}$$

$$y(t) = \begin{bmatrix} C & 0 \end{bmatrix} \begin{bmatrix} x(t) \\ z(t) \end{bmatrix},$$

or, simply

$$\bar{x}(t) = \bar{A}\,\bar{x}(t) + \bar{B}\,u(t)$$
$$y(t) = \bar{C}\,\bar{x}(t), \tag{3}$$

where $\bar{x}(t) = \begin{bmatrix} x(t) & z(t) \end{bmatrix}^{T}$.

The state space model then becomes controllable, so it is possible design an optimal control law $u(t) = -K \bar{x}(t)$ using the linear quadratic regulator (LQR) theory. In this work, the LQR design is performed in frequency domain by means of the Kalman Identity (Doyle, 1981). Use of this identity makes possible to obtain the penalty matrices $Q = C_C^T C_C$ and $R = \rho I$ that lead approximately to the pre-specified frequency response.

An approximation for the Kalman Identity, where the free parameters are Cc and ρ, is given by:

$$\sigma_i \left(G \right) \cong \frac{1}{\sqrt{\rho}} \cdot \sigma_i \left[C_c \left(\omega I - \bar{A} \right)^{-1} \bar{B} \right], \tag{4}$$

where $G(s) = K \left(I - \bar{A} \right)^{-1} \bar{B}$. Choosing

$$C_C = \left[-C_2 C A^{-1} \quad -\left(C A^{-1} B \right)^{-1} \right], \tag{5}$$

the frequency response will exhibit a constant decay ratio of -20dB/dec, since

$$C_C \left(I - \bar{A} \right)^{-1} \bar{B} = \left[-C_2 C A^{-1} \quad -\left(C A^{-1} B \right)^{-1} \right] \begin{bmatrix} \left(I - A \right)^{-1} & 0 \\ \dfrac{C}{s} \left(I - A \right)^{-1} & \dfrac{I}{s} \end{bmatrix} \begin{bmatrix} B \\ 0 \end{bmatrix} = \frac{1}{s}. \tag{6}$$

Note that ρ remains as the unique parameter for adjusting the frequency response. Once the decay ratio is also -20dB/dec around the crossover, there is some robustness associated to the design (Cruz, 1996).

In his work, Mukhopadhyay (1978) shows the equivalence between the PID control law, given by

$$u(t) = -kp\, y(t) - ki \int_0^t y(t)dt - kd \frac{dy(t)}{dt}, \tag{7}$$

and the complete state feedback control law of a system augmented with integrators to its output is given by

$$u = -\bar{k}p.x - \bar{k}i. \int_0^t ydt \ . \tag{8}$$

The author shows that the inverse, or in other words, the mapping of Equation (8) in the PID structure of Equation (7), is only possible when the number of outputs is exactly half of the number of states. However, it is possible to obtain an approximate solution, in the least square sense, using a pseudo-inverse or generalized inverse (Noble, 1977). The equivalences are given by

$$\left[kp \quad kd \right] = \bar{k}p. \begin{bmatrix} C \\ C.A - C.B.\bar{k}p \end{bmatrix}^{-1} \tag{9}$$

And

$$ki = \left(I + kd.C.B \right) \bar{k}i \ . \tag{10}$$

In this case, system order is 7, much more than order 2, and, therefore, one will reach just an approximate behavior. The achieved PID parameter values are

$$kp = 1330,2$$
$$ki = 3250,1$$
$$kd = 34,4$$

Since the PID control law is just an approximation of the state feedback control law, the frequency response diagram should be verified *a posteriori*. Figure 9 shows the frequency response plots for comparing the LQR to the PID controller. Note that the crossover frequency was increased and the decay ratio in the high frequencies was reduced. In any way, even with PID, the robustness can be considered reasonable once the system exhibits 16 dB of gain margin and 66 degrees of phase margin.
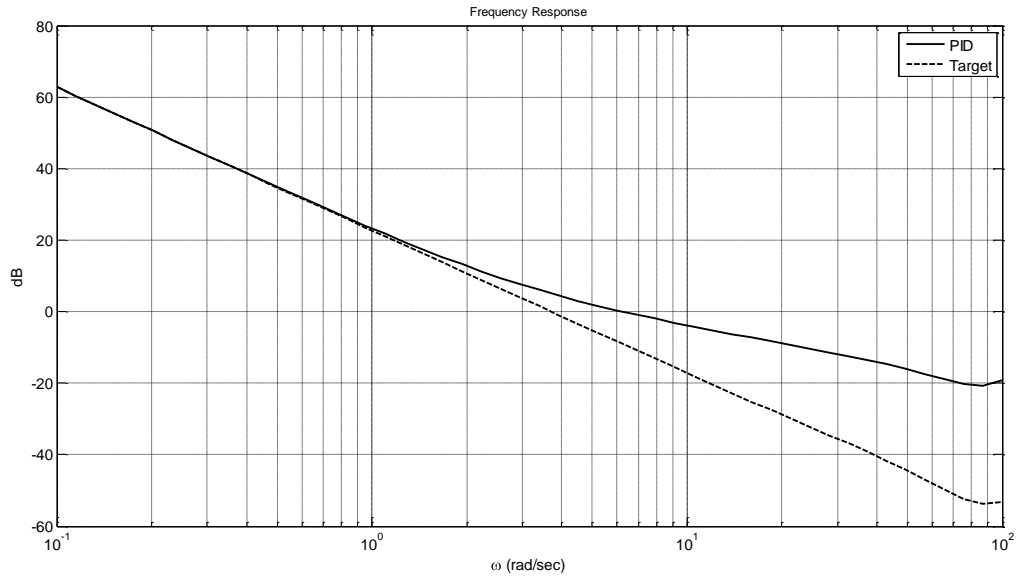

Figure 9 – Frequency response (LQR x PID).

Figure 10 shows the closed loop Bode diagram. From this figure, it is clear that the system results underdamped with a stopband of 1 Hz, approximately.
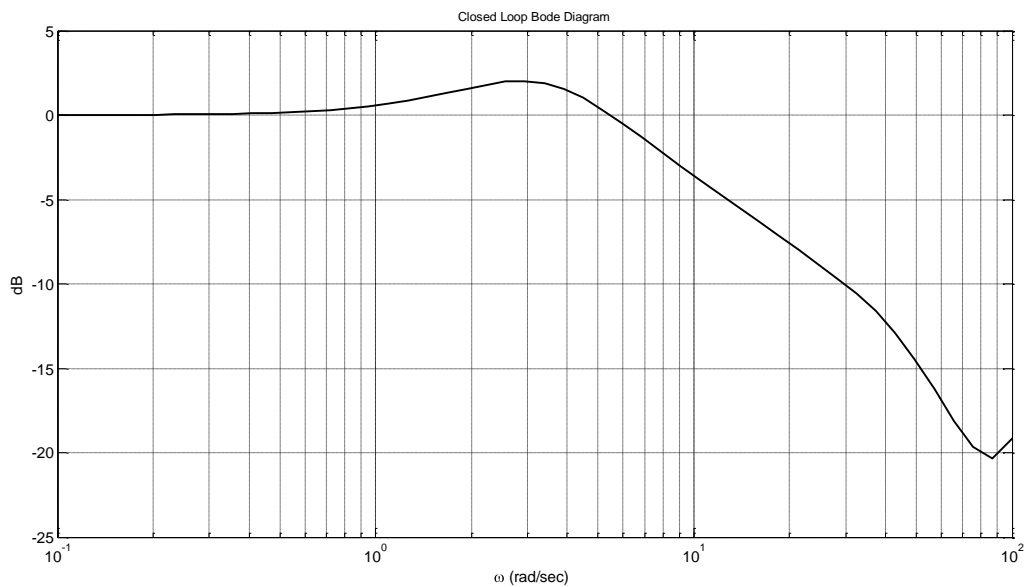

Figure 10 – Closed loop frequency response.

The time domain performance of the PID controller is shown in figure 11 and 12. A reference signal filtered by the function F(s) has been used in the input in order to reduce the overshoot whenever the setpoint is abruptly changed. A step change of 0,1 rad ($\approx 5,7°$) in the setpoint has been applied at the simulation start and a 10V step disturbance has been added to the control signal after 5 sec in order to represent a constant torque wind.

$$F(s) = \frac{1}{(0.35s + 1)^2} \, ,$$

(11)

Because of the filtering block in the reference sign, the radar system takes about 1.5 sec in order to the antenna position accommodates in its new value. On the other hand, the load disturbance is rejected at the steady state and the antenna positioning is reestablished in about 1 sec.
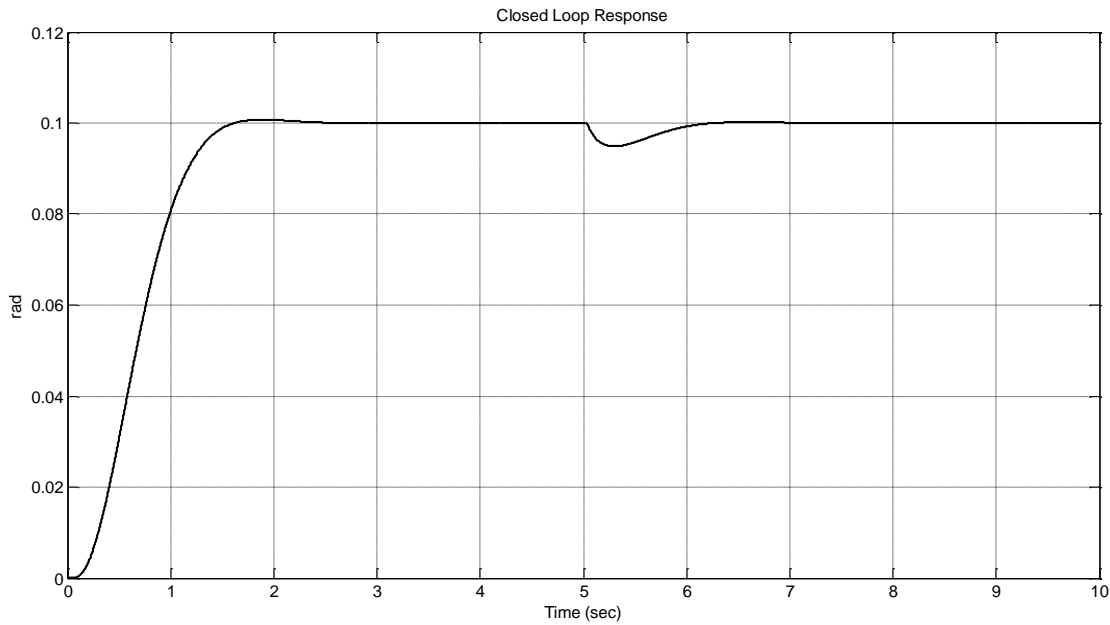

Figure 11 – Time domain performance of the PID controller.

Figure 12 shows the control effort necessary during the maneuver described with the reference signal and for the rejection of the step type signal. The maximum voltage applied to the DC motor, about 28 Volts, suggests that PID controller design is compatible with the physical constraints of the problem.
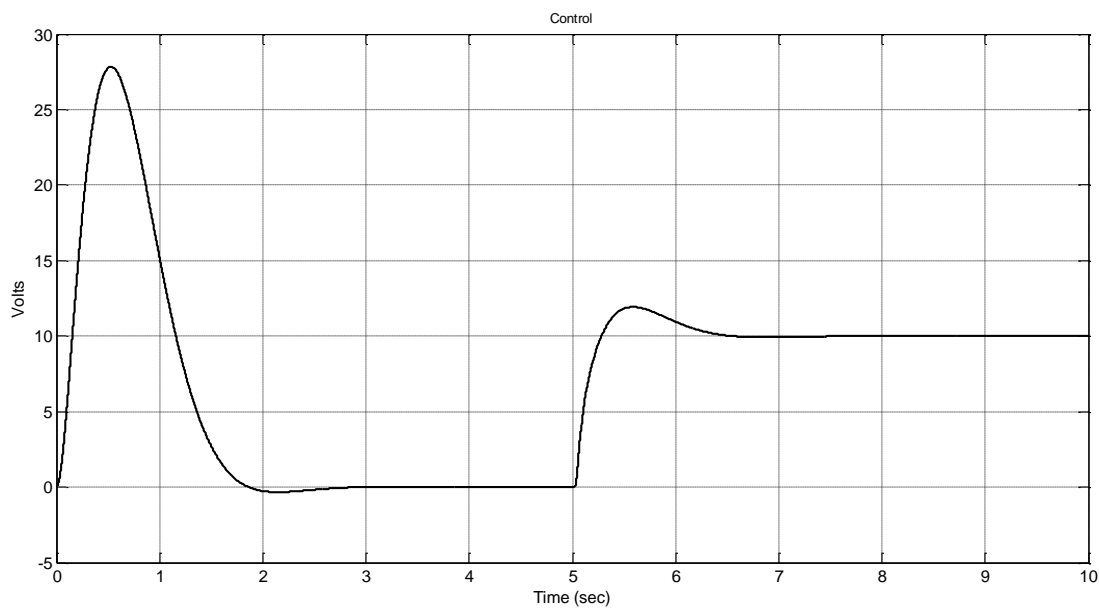

Figure 12 – Control effort.

To evaluate the parametric robustness of the designed control system, random changes in all model parameters have been made and simulated. Time domain responses remained quite satisfactory even in these cases.

6. CONCLUSION

This work has shown some relevant aspects of the mechatronics design of a large radar-antenna set for weather applications. Although the control system seems to be the core of the radar design, control design is but one of the main concerns related to a consistent project (Armellini, 2006).

For this prototype system, cheap controllers, as a PID or a LQR strategy, could be designed and implemented. The approach described in this paper allowed the transformation of a LQR controller to a high performance PID controller.

The prototype is operating at the test site but many things remain to be proceeded as the structural analysis and the field control experiments. Field data acquired after installation of the weather radar on the tower is strongly disturbed by tower harmonics, which turns the carrying on of experiments no elementary task.

7. ACKNOWLEDGEMENTS

8. REFERENCES

Armellini, F.: 2006. Projeto e Implementação do Controle de Posição de uma Antena de Radar Meteorológico através de Servomecanismos. Dissertação de Mestrado, Departamento de Engenharia Mecânica, Escola Politécnica da USP, 123p.

Baek, J. H.: 2006. Modeling on a Gimbal with an Antenna and Investigation on the Influence of Backlash, JSME Int Journal, Series C, Vol. 49, No.3, p804-813

Da Cruz, J. J.; 1996, "Controle Robusto Multivariável", Ed. USP, 163p.

Doyle, J. C.; Stein, G.; 1981, "Multivariable Feedback Design: Concepts for a Classical / Modern Synthesis", *IEEE Transactions on Automatic Control*, 26, pp. 4-16.

Houpis, C. S.; Rasmussen, S. J., 1999, "Quantitative feedback theory", Dekker

Gawronski, W.; 2006, Servo Performance Parameters of the Deep Space Network Antennas, IPN Progress Report 42-167.

Mukhopadhyay, S.; 1978, "P.I.D. Equivalent of Optimal Regulator". *Electronics Letters*, Vol. 14, No. 25, p.821-822.

Noble, B.; Daniel, J. W., 1977, Applied Linear Algebra, Prentice-Hall.

9. RESPONSIBILITY NOTICE

The authors are the only responsible for the printed material included in this paper.